Published in final edited form as:
Biomaterials. 2014 September ; 35(28): 8113–8122. doi:10.1016/j.biomaterials.2014.06.004.

Engineering biodegradable polyester elastomers with antioxidant properties to attenuate oxidative stress in tissues

R. van Lith[a], **E.K. Gregory**[b,d], **J. Yang**[a], **M.R. Kibbe**[b,d], and **G.A. Ameer**[a,b,c,d,*]

[a]Biomedical Engineering Department, Northwestern University, Evanston, IL 60208, USA

[b]Department of Surgery, Feinberg School of Medicine, Northwestern University, Chicago, IL 60611, USA

[c]Chemistry of Life Processes Institute, Northwestern University, Evanston, IL 60208, USA

[d]nstitute for BioNanotechnology in Medicine, Northwestern University, Chicago, IL 60611, USA

Abstract

Oxidative stress plays an important role in the limited biological compatibility of many biomaterials due to inflammation, as well as in various pathologies including atherosclerosis and restenosis as a result of vascular interventions. Engineering antioxidant properties into a material is therefore a potential avenue to improve the biocompatibility of materials, as well as to locally attenuate oxidative stress-related pathologies. Moreover, biodegradable polymers that have antioxidant properties built into their backbone structure have high relative antioxidant content and may provide prolonged, continuous attenuation of oxidative stress while the polymer or its degradation products are present. In this report, we describe the synthesis of poly(1,8-octanediol-co-citrate-co-ascorbate) (POCA), a citric-acid based biodegradable elastomer with native, intrinsic antioxidant properties. The *in vitro* antioxidant activity of POCA as well as its effects on vascular cells *in vitro* and *in vivo* were studied. Antioxidant properties investigated included scavenging of free radicals, iron chelation and the inhibition of lipid peroxidation. POCA reduced reactive oxygen species generation in cells after an oxidative challenge and protected cells from oxidative stress-induced cell death. Importantly, POCA antioxidant properties remained present upon degradation. Vascular cells cultured on POCA showed high viability, and POCA selectively inhibited smooth muscle cell proliferation, while supporting endothelial cell proliferation. Finally, preliminary data on POCA-coated ePTFE grafts showed reduced intimal hyperplasia when compared to standard ePTFE grafts. This biodegradable, intrinsically antioxidant polymer may be useful for tissue engineering application where oxidative stress is a concern.

*Corresponding author. g-ameer@northwestern.edu.

1. Introduction

The biocompatibility of implantable materials has evolved in the past decades from simply meaning inertness, via the lack of a deleterious response, to the current Williams' definition of "the ability of a biomaterial to perform its desired function without eliciting any undesired effect, but generating a beneficial cellular or tissue response" [1]. Our increased understanding of the biological responses to synthetic materials has led to this change of viewpoint. An important component of a biomaterial's response that can have an impact on the performance of medical devices yet is often overlooked in the biomaterials science community is oxidative stress. When a biomaterial induces an inflammatory response, leukocytes release various cytokines and chemokines and generate reactive oxygen species (ROS) (e.g., superoxide, hydroxyl radicals and hydrogen peroxide) [2]. Pro-oxidant molecules and compounds react with and damage DNA, proteins and lipids, potentially impairing the normal function of cells. Indeed, the detection of ROS is currently being used to characterize the inflammatory host tissue response to biomaterials, both *in vitro* and *in vivo* [3]. The induction or presence of oxidative stress is particularly relevant to biodegradable polymers such as polylactides, as the local accumulation of polymer degradation products generate ROS [4, 5]. In fact, excess ROS is a significant cause of toxicity for many biodegradable materials [6–9].

Oxidative stress may also be a pathophysiological response due to an imbalance between the production of oxidants and the antioxidant defense mechanism, resulting in a net increase in ROS [10]. For example, oxidative stress has been implicated in the progression of atherosclerosis [11, 12] and restenosis, the major cause of failure of vascular interventions [13, 14]. Specifically, excessive ROS lead to overproliferation of vascular smooth muscle cells [15–17]. Therefore, biomaterials that can counter the effects of oxidative stress and inhibit excessive ROS generation in a sustained manner may be a useful tool for therapies that target these medical problems.

Previous attempts to limit biomaterial-induced oxidative stress included synthesizing polymers that lead to charge-neutral degradation products [18], which does not inhibit oxidative stress induced by other factors, and conjugating antioxidant molecules to the surface of the biomaterial to provide local antioxidant therapy [19–21]. Examples of the latter include the conjugation of small molecule antioxidants such as superoxide dismutase mimetics (mSOD), vitamin E, gallic acid, catechin, ascorbic acid and glutathione to ultra-high molecular weight poly(ethylene) (UHMPE), poly(acrylic acid), gelatin, poly(methyl methacrylate) and poly(ethylene glycol) [22–26]. Although this strategy has resulted in some suppression of oxidative stress, it results in materials that have low relative antioxidant mass. Biodegradable polymers with native intrinsic antioxidant properties may therefore provide the benefit of relatively high antioxidant content and continuous local antioxidant potential while the polymer is present. Recently such a polymer with intrinsic antioxidant capacity was synthesized [27], but despite some inhibition of ROS generation in cells, no specific effects on free radicals or excess metals, specifically iron were reported. Moreover, the authors did not report *in vivo* evidence of a functional effect of their material.

Our laboratory has previously described the synthesis and characterization of polydiolcitrates (PDC), biodegradable non-toxic polyesters that have been shown to be useful for several tissue engineering applications [28–31]. Herein we demonstrate that these polymers can be easily engineered to have enhanced, biologically relevant antioxidant activity by incorporating ascorbic acid (AA) into the polymer network (Figure 1). Ascorbic acid is a safe and natural antioxidant that has several hydroxyl moieties that can participate in a polycondensation reaction. Citric acid, a metal chelator, is a stabilizer of AA and was expected to protect AA during the reaction conditions for the prepolymer synthesis [32–34]. The inclusion of metal-chelating citric acid is important as transition metals such as iron are well-known factors in oxidative stress, particularly involved in the Fenton reaction and implied in many ROS-related conditions [35, 36]. Moreover, ascorbic acid can act as a pro-oxidant in the presence of free transition metals [37], highlighting the need for metal chelating properties. We hypothesized that these degradable poly(diolcitrate-co-ascorbate) polyesters would have both direct and indirect antioxidant properties due to the radical scavenging ability of AA and iron chelation activity of citric acid and that the copolymer would protect cells from oxidative stress conditions. Furthermore, we hypothesized that inhibition of ROS would selectively inhibit vascular smooth muscle cell proliferation and therefore result in the inhibition of neointimal hyperplasia.

2. Materials and Methods

2.1 Reagents

All chemicals were purchased from Sigma and used without further purification except where indicated otherwise.

2.2 Polymer synthesis

Poly(1,8 octanediol-co-citrate-co-ascorbate) (POCA) was synthesized by mixing 1,8-octanediol, citric acid and ascorbic acid at a ratio of 5:5:1 and heated at 160°C for 10 minutes, followed by 140°C for an additional 60 minutes. Increasing the relative amount of ascorbate further led to the formation of a viscous liquid rather than a solid elastomer, but a viscous liquid that lacked structural integrity (data not shown). POC was synthesized as a reference polymer by copolymerizing 1,8-octanediol and citric acid in equimolar amounts. After prepolymerization, prepolymers were dissolved in ethanol and purified by precipitation in 5× excess distilled water (MQ, Millipore, Billerica, MA). The resulting purified prepolymer precipitate was lyophilized for 3 days. Prepolymers were subsequently post-polymerized for 4 days at 80°C for all experiments. After post-polymerization, polymers were gas sterilized with ethylene oxide gas according to manufacturer's instructions (Anprolene AN74i, Andersen Products, Haw River, NC). DMEM cell culture media was added to sterilized polymers to leach out acidic products at 37°C, with replacement of media upon yellow discoloration. When no more discoloration for at least one day was observed, the polymer was rinsed 3× with phosphate buffered saline (PBS) and used for cell culture experiments. For other *in vitro* experiments, polymers were washed thoroughly with MQ water and lyophilized before use.

2.3 Polymer characterization

Tensile testing was performed according to American Society for Testing and Materials (ASTM) 412A on an Instron 5544 equipped with 500-N load cell (Instron, Norwood, MA). Briefly, dumbbell-shaped samples were pulled to failure at a rate of 500 mm/min. Young's modulus and maximum loads were obtained from stress–strain data. The polymers' density ρ was measured using the liquid displacement test using ethanol as test liquid. The crosslink density *n* was calculated using equation (1) [38]:

$$n=\frac{E_0}{3RT}=\frac{\rho}{M_c} \quad (1)$$

Where *n* represents the number of active network segments; M_c the molecular weight between crosslinks; R the universal gas constant (8.3144 J mol-1 K-1); T the absolute temperature (K) and E_0 the Young's modulus.

The proton nuclear magnetic resonance (NMR) spectrum of prepolymers was recorded with an Ag500 NMR spectrometer (Bruker, Billerica, MA) at ambient temperature, using dimethylsulfoxide-*d6* as solvent, and trimethylsilane as the internal reference. The spectra were obtained with a free induction delay resolution of 0.157 Hz/point, corresponding to a sweep width of 10.33 kHz, acquisition time was 3.17 s.

Fourier transform infrared (FT-IR) transmission spectra were recorded in attenuated total reflectance mode on a Nicolet Nexus 870 spectrometer (Thermo Scientific, Waltham, MA) by accumulation of 32 scans, with a resolution of 8 cm^{-1}. Matrix-assisted laser desorption/ionization (MALDI) was performed on POC and POCA prepolymer solutions, as well as supernatants after several hours of incubation of polymer films in MQ at 37°C. For supernatants, solutions were directly plated without use of a matrix using a matrix-free laser desorption/ionization (LDI-MS) method. For prepolymer solutions, diluted solutions were used in a matrix of cinnamic acid in tetrahydrofuran (THF) (10 mg/mL) at a 1:10 ratio, final polymer concentration of 3 mg/mL. Spectra were collected with a 4800 MALDI-TOF/TOF mass spectrometer (Applied Biosystems, Foster City, CA). A 355 nm Nd:YAG laser was used as a desorption/ionization source, and all spectra were acquired with 20 kV accelerating voltage using positive reflector mode. The weight-average and number-average molecular mass of pre-POC and pre-POCA was measured by MALDI-MS. The peaks from the main distribution and all the sub-distributions were taken in consideration in the calculation of molecular weight of the pre-polymers. The intensity threshold for inclusion of peaks was set to 1%, while spectra were corrected for matrix-specific peaks.

2.4 Intrinsic antioxidant activity

2.4.1 Free radical scavenging—To test the free radical scavenging capacity of POC and POCA, the scavenging of both a hydrophilic radical cation (2,2'-azino-bis(3-ethylbenzthiazoline-6-sulphonic acid (ABTS)) and a lipophilic radical (1,1-diphenyl-2-picrylhydrazyl (DPPH)) was monitored. For ABTS, a stock solution of 7 mM ABTS and 2.45 mM sodium persulfate in MQ water was prepared and left for 16 hours in the dark at room temperature, after which the solution was sequentially filtered with 5, 1 and 0.45 um filters. This working solution was then exposed to the polymers (50 mg/mL) and incubated

at 37°C. At each time point, ABTS solution was sampled, diluted with MQ water 1:1 and the absorbance measured at 734 nm. All measurements were performed in triplicate. The antiradical activity was measured as % inhibition of free radicals by measuring the decrease in absorbance compared to control solutions. For DPPH, a 400 μM solution of DPPH in ethanol was prepared. Lyophilized polymers were placed in DPPH solution (50 mg/mL) and incubated at 37°C. DPPH free radical content was me asured by monitoring the absorbance changes at 517 nm at each time point. All determinations were performed in triplicate. The antiradical activity was measured as % inhibition of free radicals by measuring the decrease in absorbance compared to control solutions.

2.4.2 Iron chelation—The inhibition of iron chelation activity was assessed by incubating polymers with 0.25 mM $FeCl_2 \cdot 4H_2O$ solution (50 mg/mL) at 37°C. Supernatants were collected at each time point and reacted with 5 mM ferrozine indicator solution in a 5:1 ratio. Ferrous ions chelated by polymers will not be available for ferrozine reaction, resulting in lower color development. Absorbance was measured at 534 nm.

2.4.3 Lipid peroxidation inhibition—The antioxidant activity of polymers was evaluated using the β-carotene-linoleic acid assay with a few modifications described below [39]. Briefly, tween 40 (4 g), β-carotene (4 mg) and 0.5 mL linoleic acid were mixed in 20 mL chloroform. After removing chloroform in a rotary evaporator, 30 mL of pre-warmed Britton buffer (100 mM, pH 6.5) was added to 1 mL of the oily residue with vigorous stirring. Aliquots (1 mL) of the obtained emulsion were added to polymers (50 mg). Reaction mixtures were incubated at 45°C for 100 minutes. Spontaneous oxidation of linoleic acid at 45°C leads to β-carotene discoloration, which was monitored by the decrease in absorbance at 470 nm, starting immediately after sample preparation (t = 0 min).

2.5 Cell viability and proliferation

To assess biocompatibility of polymers with vascular cells, 48-well plates were coated with 80 μL of polymer solution (30% w/w in ethanol), the ethanol evaporated and plates post-polymerized at 80°C for 4 days, resulting in approximately 20 mg polymer/well. After gas sterilization and acid leaching, plates were pre-treated with each cell type's respective growth media (EGM-2 for HUVECs and SmGM-2 for HASMCs, respectively). Human umbilical vein endothelial cells (HUVECs, Lonza, Walkersville, MD) and human aortic smooth muscle cells (HASMCs, Lonza, Walkersville, MD) were then seeded in wells at a concentration of 5000 cells/cm^2. Cells of passage 4–8 were used for all experiments. Viability of both cell types was assessed by staining with Live/Dead assay (Life Technologies, Carlsbad, CA) according to manufacturer's instruction after 5 days of culture. For proliferation assessment, the total DNA content in each well was measured over time with the commercial picogreen reagent (Life Technologies, Carlsbad, CA). At each time point, cells were rinsed 3× with PBS, and 150 μL of PBS containing 1% Triton-X was added to wells. After 15 minutes of lysing cells at 37°C, supernatant was collected and combined in 1:1 ratio with picogreen. A standard curve was generated with cells in regular maintenance culture. The standard curve was used to calculate number of cells based on picogreen fluorescence.

2.6 Oxidative stress in cells

To assess the reduction of cellular oxidative stress upon an oxidative challenge, HUVECs were incubated with polymers for 2 hours at 37°C by placing the polymer into transwell inserts. Then, inserts with polymers were removed, and cells were incubated with 5-(and-6)chloromethyl-2′,7′dichlorodihydrofluorescein (DCF, 10 μM) for 30 minutes, washed 3× with warm Hank's buffered saline solution (HBSS) and subsequently challenged with hydrogen peroxide (200 μM in HBSS). Fluorescence development was monitored at Ex/Em 485/535 nm.

To measure the polymers' effect on cell viability upon an ROS challenge, cells were cultured on POC and POCA-coated plates as before. Upon reaching confluence, cells were treated with 50 μM menadione, known to induce rapid cell death due to excessive ROS generation [40]. After exposure to menadione, cells were monitored over time with light microscopy and stained with Calcein-AM to assess viability. Background autofluorescence correction was performed during post-processing in ImageJ with rolling ball radius of 200. All images were then equally adjusted to midtone level of 0.8 and highlight level of 50 using Adobe Photoshop CS5. Viability was quantified by counting of percentage calcein-positive cells.

2.7 *In Vivo* neointimal hyperplasia: guinea pig aortic interposition model

2.7.1 Fabrication of the POCA ePTFE Graft—POCA-ePTFE grafts were fabricated from ePTFE grafts (Inner diameter: 1.52±0.05 mm, intermodal distance: 25±10 μm, wall thickness:101.6±25.4 μm, Zeus Inc., Orangeburg, SC). ePTFE grafts were coated with a 10% w/w polymer in ethanol solution using infusion coating followed by ethanol evaporation. This process was repeated once, after which coated grafts were post-polymerized at 80°C for 4 days. This coating process, developed in our laboratory, leads to a polymer-content of 20.1±3.8%, or approximately 1.4–1.6 mg ascorbic acid per 100 mg POCA-ePTFE. This polymer coating does not significantly change the node-and-fibril architecture of grafts or graft compliance (supporting data S8 and S9). Grafts were then gas-sterilized and acid-leached. Prior to implantation, grafts were washed with 70% ethanol (3×), the ethanol was evaporated and grafts kept in PBS.

2.7.2 Animal Surgery—All animal procedures were performed in accordance with the Guide for the Care and Use of Laboratory Animals published by the National Institutes of Health (NIH Publication 85-23, 1996) and approved by the Northwestern University Animal Care and Use Committee. An aortic interposition graft was performed on eight 10–12 week old Adult male Hartley guinea pigs between 650 and 750 g. Animals were anesthetized with isoflurane (1.5–5%) and treated preoperatively with carprofen subcutaneously 2 mg/kg for pain control. Via a 3 cm midline incision the abdominal aorta was dissected just distal to the renal arteries to the bifurcation of the iliac arteries. Heparin 400 u/kg was given subcutaneously and allowed to circulate 20 minutes prior to cross clamping of the aorta. After obtaining proximal and distal vascular control approximately 1 cm portion of the aorta was removed and the graft implanted. The proximal and distal anastomoses were fashioned utilizing a 9-0 ethilon suture via 12 interrupted sutures. Just prior to completion of the distal anastomosis, the distal then proximal clamps were flashed to evacuate all clots and air and

the graft was then flushed with 10 ml of 1% heparinized saline. After completion of the distal anastomosis the cross clamps were removed, first distally then proximally. Surgicel was utilized to obtain hemostasis. Graft patency was confirmed by presence of a pulse in the distal aorta. Once hemostasis was achieved the abdomen was closed in 2 layers using 4-0 vicryl to close the abdominal wall and 4-0 ethilon to approximate the skin. Groups included ePTFE and POCA-ePTFE. At 4 weeks the animals were anesthetized and euthanized via bilateral thoracotomies. After *in situ* perfusion-fixation with PBS (500 ml) and 2% paraformaldehyde (500 ml) via a cannula inserted into the left ventricle, the graft was harvested *en bloc* along with 5 mm of the proximal and distal aorta.

2.7.3 Specimen Processing—The specimen was divided mid-graft into proximal and distal sections which were cryopreserved with 30% sucrose and frozen. Specimens were examined qualitatively for histologically evidence of neointimal hyperplasia using 5-μm hematoxylin and eosin (H&E)-stained cross sections at the level of the graft. Digital images of stained section were collected with light microscopy using a Zeiss Imager-A2 microscope (Hallbergmoos, Germany).

2.8 Statistical Analysis

Statistical analysis was performed using Microsoft® Excel software and Graphpad Prism 5.0 (Graphpad Software Inc., USA). Data from independent experiments were quantified and analyzed for each variable. Comparisons between two treatments were made using student's T-test (two tail, unequal variance) and comparisons between multiple treatments were made with analysis of variance (ANOVA), with Bonferroni post-hoc analysis. A value of $p < 0.05$ was considered to be statistically significant.

3. Results and Discussion

3.1 Polymer characterization

The Young's moduli, polymer density and molecular weight between crosslinks did not differ significantly between POC and POCA and were in good agreement with previously published values for POC (Table 1) [41, 42]. Moreover, the incorporation of ascorbic acid did not significantly alter the available free carboxylic acid groups or polymer hydrophilicity (supplemental data S1). The hydrolytic degradation rate also was not affected by incorporation of ascorbic acid, with polymer discs losing structural integrity after 2 months of incubation in PBS at 37°C, when approximately 25% mass loss had occurred (supplemental data S1). The substantial equivalence between POCA and POC is important to note, since POC has been shown to have favorable properties for both *in vitro* and *in vivo* compatibility of devices, as well as tissue engineering applications [28, 29, 31, 41].

For NMR analysis, except for the peaks at 2.5 ppm (-CH_2- from citric acid) and multiple peaks at 1.2 ppm (-$CH_2CH_2CH_2$- from octanediol) of POC prepolymer, the presence of the characteristic peaks at 3.6 ppm (-CH_2OH from 6), 3.8 ppm (-CHO- from 8) and 4.1 ppm (-CHOH from 7) in the ^{1}H NMR spectra of POCA confirms the successful incorporation of ascorbic acid into POCA prepolymer (Figure 2 insert). Based on H NMR peak ratios, H NMR indicated that the final POCA product contained approx. 7–8 w/w% ascorbic acid, in

close agreement with the feed ratio of 9.4 w/w% of the reaction. We can not exclude the possibility that some ascorbic acid degraded during the initial prepolymerization step as per some visible browning of the polymer. Nonetheless, most of the ascorbic acid is preserved as indicated by the presence of a strong ascorbate-specific peak and the absence of ascorbate degradation products' (e.g. furan and methylfuran) peaks in pre- and post-polymerized POCA MALDI spectra. Ascorbic acid-specific peaks are absent from prePOCA MALDI (figure 3), but LDI-MS performed on short-term releasates from POCA shows a strong peak at 176 m/z, absent from POC releasate (Supplemental data S3). Moreover, free ascorbic acid released from POCA over time only accounted for less than 6% of the incorporated amount (Supplemental data S2). These data together indicate that ascorbic acid is incorporated as part of the polymer backbone and not present in its free form in the final, acid-leached product.

MALDI spectra further confirmed the low-molecular-mass of POC and POCA pre-polymers (Mw 915 and 917 Da, Mn 836 and 828, PD 1.09 and 1.11, respectively), in good agreement with previous results [28, 29, 41]. Characteristic spacing between clusters of peaks exist of 128 Da, 174 Da and 302 Da, corresponding to the addition of an octanediol (D), citric acid (C) or C_1D_1 segment to oligomers, respectively, with evidence of pre-polymer oligomers of up to C_5D_5 length present in the prepolymer mixture (Figure 3). Moreover, peaks could be identified of cyclic oligomers, e.g. showing a shift of −18 Da from 645.8 Da corresponding with linear $[C_2D_2+Na^+]$ to 627.8 Da, corresponding with cyclic $[C_2D_2+Na^+]$. Finally, POCA appears to show a higher intensity of Na^+ adducts than K^+ adducts, which may in actuality indicate replacement of citrate segments by ascorbate, causing a shift of −16 Da, making the prePOCA+K^+ peaks coincide with prePOC+Na^+ peaks (Figure 3). The limited release of free ascorbic acid over time, despite substantial polymer degradation, also indicates that ascorbic acid is released to a large extent as co-oligomer with citric acid and octanediol.

FTIR spectra show minor differences between POC and POCA as expected. Peaks at wavelengths of 1730 cm^{-1} (polyester C=O stretch) and 1190 cm^{-1} (C-O) in the IR show the formation of polyester bonds. The broad peak around 1450 cm^{-1} in POCA is indicative of asymmetric C=C-C in ascorbic acid, while the small peak at approximately 1650 cm^{-1} was assigned to the C=C ring stretching of ascorbic acid (Figure 4) [43]. The lactone C=O in ascorbic acid overlaps with and is obscured by the strong polyester peak at 1730 cm^{-1}. Overall, FTIR spectra are indicative of ring structures of ascorbic acid still being intact upon incorporation into the backbone.

3.2 Antioxidant Properties

POC and POCA show significant direct and indirect antioxidant capacity, although POCA was stronger. POCA, as expected by virtue of its incorporated ascorbic acid, showed rapid free radical scavenging activity as per DPPH (lipophilic) and ABTS (hydrophilic) assays (Figure 5A and B) with 100% radicals scavenged within 24 hours. Free ascorbic acid typically scavenges both ABTS and DPPH radicals instantaneously (supplemental data S4), while scavenging by POCA increases gradually during the first 24 hours, indicative of ascorbic acid being slowly released from POCA. Interestingly, the POC itself also showed

significant radical scavenging capacity, although this was not the case for the POC releasate (supplemental data S5). Free radical scavenging activity of POC might be caused by the citric acid in its backbone structure. Although citric acid has previously been shown to scavenge radical cation N,N-dimethyl-p-phenylenediamine [44], it is not a typically reported property. Nonetheless, citric acid consistently showed scavenging activity in the DPPH assay, yet not in the ABTS assay (supplemental data S4). There may be another factor conferring radical scavenging properties to POC. The chemical structure of POC oligomer is similar to that of triglycerides [45], which have been reported to potentially have antioxidant properties. This chemical resemblance may play a role in POC's capacity to scavenge radicals [46]. Moreover, prepolymer MALDI data are indicative of cyclic oligomer species (Figure 3), which may also confer radical scavenging properties, as the ring structures in combination with pendant hydroxyl groups have been identified to confer radical scavenging properties in flavonoids. Further research is needed to confirm the exact mechanism behind POC's radical scavenging capacity. The data suggest that the additional radical scavenging ability of POCA over POC is due to ascorbic acid being released through hydrolytic degradation.

As expected, both POC and POCA show strong iron chelation properties due to their citric acid content (Figure 5C). Interestingly, POCA showed increased metal chelation over POC, despite the equal contents of citric acid. Although ascorbic acid has limited iron chelation potential itself [47], the incorporation of ascorbic acid might increase the accessibility of citric acid's carboxylic and hydroxyl groups for iron coordination bonds, leading to a synergistic effect.

Lipid peroxidation was strongly inhibited by POCA as assessed by the β-carotene bleaching assay (Figure 5D). After 100 minutes of heating at 45°C, exposure to POCA led to almost complete abolishment of lipid peroxidation. POC, in contrast, showed only modest prevention of lipid peroxidation (Figure 5D). The known role of iron in lipid peroxidation [39] explains why POC, as an iron chelator, partially inhibits lipid peroxidation.

Since these polymers are biodegradable and the antioxidant activity is expected to be a lasting attribute of their backbone structure, we evaluated whether partially degraded POC and POCA retains antioxidant capacity. Indeed, after 1 month of incubation in PBS at 37°C, both POC and POCA retain ed most of their iron chelating and free radical scavenging capacity. The inhibition of lipid peroxidation, on the other hand, although still present, was decreased to 14.7±1.1% and 21.9±5.8% of that measured using pristine POC and POCA, respectively, at 100 minutes (supplemental data S6).

3.3 Cell viability and proliferation

Culture of both HUVECs and HASMCs did not result in any significant cytotoxic effect, as per high cell viability (Figure 6, top) and spreading observations. As observed before, HUVECs tended to exhibit a more elongated phenotype on both POC and POCA [30]. HASMC proliferation was significantly lower on both polymers, with a 18.1±3.2% and 52.3±7.2% reduction at 3 days and a 15.6±0.9% and 40.5±3.5% reduction at 5 days for POC and POCA, respectively (Figure 6, bottom). The significant reduction of cell proliferation on POCA particularly is a highly desirable effect when considering the potential use of POCA

as a coating in vascular grafts to prevent neointimal hyperplasia. These results corroborate the *in vitro* antioxidant activity found for both polymers, and, as expected, the reduction of ROS inhibits HASMC proliferation [15, 17]. We previously reported that ascorbic acid can also lead to increased proliferation of smooth muscle cells at concentrations of 0.5–1 mM [48], likely due to a pro-oxidant effect at those concentrations [49]. Current results also confirm that the ascorbic acid levels present in POCA are low enough to not lead to an increase in HASMC proliferation. Further, the chelation of transition metals by POCA will also prevent the potential pro-oxidant effect of low levels of ascorbic acid. HUVEC proliferation, on the other hand, was not hampered and even slightly increased at 5 days on POC and POCA. These results are also consistent with the work of Ulrich-Merzenich et al., who previously showed the opposite effects ascorbic acid has on human vascular ECs and SMCs [50].

3.4 Oxidative stress in cells

Exposing cells to hydrogen peroxide increases intracellular levels of ROS, leading to increased oxidative stress as measured through DCF fluorescence (Figure 7) [51, 52]. Cells were cultured on TCP and exposed to the polymers for two hours through transwell inserts, after which cells were stimulated or not with hydrogen peroxide. In non-stimulated cells, oxidative stress remains low over time, as expected (Figure 7A). There was a slight reduction in basal levels for POC and POCA ($P=0.012$ and 0.008 for ePTFE vs. POC and ePTFE vs. POCA, respectively), suggesting not just a protective effect from oxidative challenges, but also a basal oxidative status-modulating effect of both polymers. No difference in basal ROS was observed between POC and POCA ($P=0.151$). The observed reduction in DCF fluorescence in non-stimulated cells is consistent with previous observations by others whereby basal levels of oxidative stress in endothelial cells in culture were increased due to insufficient concentrations of ascorbic acid [53]. For cells exposed to hydrogen peroxide, oxidative stress increase relative to baseline values is minimal for both POC and POCA groups (Figure 7B). In contrast, cells exposed to ePTFE demonstrated increased oxidative stress levels relative to baseline within five minutes and relative to POC and POCA groups ($P=0.013$ and 0.007 for ePTFE vs. POC and ePTFE vs. POCA, respectively). The rapid increase of oxidative stress within the first 10 minutes as measured through DCF fluorescence upon hydrogen peroxide exposure is consistent with previous reports [52].

To further assess the protective effect of POCA against excessive ROS with cells directly cultured on the polymers, HUVECs were exposed to menadione. Menadione leads to rapid intracellular ROS generation and subsequent cell death due to excessive ROS [40, 54]. When menadione was added to confluent cell layers cultured on the polymers, HUVECs on TCP showed reduced viability after 30 minutes and cells started to detach, with markedly reduced viability and considerable cell detachment after 1 hour (Figure 8) However, cells on POC and POCA preserved their morphology, with only minor cell detachment after 60 minutes. The percentage of viable cells after 60 minutes was significantly different between TCP and POC ($p=0.031$) and TCP and POCA ($p=0.002$), but not between POC and POCA ($p=0.714$). It has been previously described that ascorbic acid levels between 50–350 μM reduce oxidative stress levels in cultured endothelial cells [55]. Moreover, in our experience,

free ascorbic acid concentrations of 125–500 μM prolongs viability of cultured HUVECs after exposure to 50 μM menadione for 1 hour (supplemental data S7). With a POCA content of 20 mg/well, maximum ascorbic release rate of 0.47 μg/mg/day (supplemental data S2) and 500 μL of media/well refreshed every 1 or 2 days, this would lead to maximum ascorbic acid concentrations of 107–214 μM, within the range reported to reduce oxidative stress. An additional mechanism that may be at play is metal chelation, as it has been shown that chelating iron can reduce oxidative stress [56–59] hence the polymer network itself also may contribute to cellular protection by limiting free iron.

3.5 *In vivo* neointimal hyperplasia: guinea pig aortic interposition model

Excessive ROS and accompanying oxidative stress are an important part in the etiology of atherosclerosis and restenosis [11–14]. Therefore, antioxidant therapy might be a useful strategy to inhibit these processes. Oral supplementation of antioxidants has been attempted for many years, yet clinical trials results have been conflicting or largely unsuccessful [60, 61]. However, the majority of trials utilized systemic administration, where reaching clinically effective concentrations may not be possible due to compound inactivation or absorption limits. However, localized administration of antioxidants has led to positive results, for example of sucinobucol after balloon angioplasty [62] and of tetradecylthioacetic acid from stents [63]. Local, targeted antioxidative gene therapy has also shown promising results [64–66]. Therefore, localized prolonged antioxidant activity through biodegradable polymers with backbone intrinsic antioxidant activity may reduce neointimal hyperplasia by decreasing initial ROS generated upon injury. Due to its superior antioxidant properties as well as strongest antiproliferative effects on vascular SMCs, POCA was used for a preliminary assessment of the *in vivo* functionality of antioxidant polymers. ePTFE grafts coated with POCA were used in a guinea pig aortic graft interposition model to assess effects on neointimal hyperplasia formation. Non-coated ePTFE grafts, which are used in standard care, were used as a reference for comparison. The guinea pig was chosen, because like humans they do not have the capability to synthesize their own ascorbic acid, contrary to all other animals except for bats and primates [67]. Moreover, ascorbic acid has been shown in both humans and guinea pigs to have an inhibiting effect on vascular SMC proliferation, depending on concentration [50, 68]. Polymer-coated grafts retained their typical node and fibril structure and graft compliance was not affected by the coating process (supplemental data S8 and S9). POCA also inhibited platelet adhesion, a beneficial property that was expected to improve graft thromboresistance (supplemental data S10). Neointimal hyperplasia was evident in POCA-ePTFE and ePTFE grafts, but was qualitatively reduced in POCA-ePTFE grafts only (Figure 9). Although there is a significant difference in surface hydrophilicity between POCA-ePTFE and ePTFE grafts, this difference does not account for the reduction in neointimal hyperplasia as separate experiments using POC-ePTFE grafts did not show a reduction in neointimal hyperplasia (supplemental figure S11). The hydrophilicity of POC and POCA is similar (supplemental data S1). These results are a preliminary confirmation that the intrinsic antioxidant capacity of POCA observed *in vitro* may translate into a desirable therapeutic outcome such as the reduction of neointimal hyperplasia in a vascular graft. In addition to antioxidant effects of POCA due to incorporated ascorbic acid, it should be noted that there is also the possibility of additional vasoprotective effects via the liberation of nitric oxide (NO) from circulating

S-nitrosoglutathione due to catalytic effects from ascorbic acid in POCA. These biological effects are currently the subject of ongoing investigation.

4. Conclusion

In conclusion, we have successfully synthesized and characterized an ascorbic acid containing polydiolcitrate with intrinsic, direct and indirect antioxidant properties. POCA exhibited strong metal chelating, free radical scavenging and lipid peroxidation inhibition properties, which are retained after 1 month of incubation in physiologic fluid. Moreover, POCA protects cells from oxidative stress effects and maintains the high viability of vascular cells, while selectively inhibiting the proliferation of smooth muscle cells. Finally, ePTFE grafts coated with POCA decrease neointimal hyperplasia in preliminary data of a guinea pig aortic graft interposition model. This new intrinsically antioxidant, biodegradable polyester may also be useful for tissue engineering applications where cellular oxidative stress is a concern.

Supplementary Material

Refer to Web version on PubMed Central for supplementary material.

Acknowledgments

This work was supported in part from funding from the National Institutes of Health (R01 EB017129-01A1, GAA; T32 HL094293-01, EKG; F32HL114255-01A1, EKG) and the American Heart Association Postdoctoral Fellowship Award (12POST12150050, EKG). FTIR measurements were performed at the Keck-II facility (NUANCE Center - Northwestern University), which has received support from the W. M. Keck Foundation, Northwestern's Institute for Nanotechnology's NSF-sponsored Nanoscale Science & Engineering Center (EEC-0118025/003), the State of Illinois, and Northwestern University. The authors would like to acknowledge Zdravka Cankova for technical support with MALDI and LDI-MS measurements.

References

1. Williams DF. On the nature of biomaterials. Biomaterials. 2009; 30(30):5897–5909. [PubMed: 19651435]
2. Juni RP, Duckers HJ, Vanhoutte PM, Virmani R, Moens AL. Oxidative stress and pathological changes after coronary artery interventions. J Am Coll Cardiol. 2013; 61(14):1471–1481. [PubMed: 23500310]
3. Selvam S, Kundu K, Templeman KL, Murthy N, Garcia AJ. Minimally invasive, longitudinal monitoring of biomaterial-associated inflammation by fluorescence imaging. Biomaterials. 2011; 32(31):7785–7792. [PubMed: 21813173]
4. Liu WF, Ma M, Bratlie KM, Dang TT, Langer R, Anderson DG. Real-time in vivo detection of biomaterial-induced reactive oxygen species. Biomaterials. 2011; 32(7):1796–1801. [PubMed: 21146868]
5. Fu K, Pack DW, Klibanov AM, Langer R. Visual evidence of acidic environment within degrading poly(lactic-co-glycolic acid) (PLGA) microspheres. Pharm Res. 2000; 17(1):100–106. [PubMed: 10714616]
6. Krifka S, Spagnuolo G, Schmalz G, Schweikl H. A review of adaptive mechanisms in cell responses towards oxidative stress caused by dental resin monomers. Biomaterials. 2013; 34(19):4555–4563. [PubMed: 23541107]
7. Li JJ, Hartono D, Ong CN, Bay BH, Yung LY. Autophagy and oxidative stress associated with gold nanoparticles. Biomaterials. 2010; 31(23):5996–6003. [PubMed: 20466420]

8. Manke A, Wang L, Rojanasakul Y. Mechanisms of nanoparticle-induced oxidative stress and toxicity. Biomed Res Int. 2013; 2013:942916. [PubMed: 24027766]
9. Matheson LA, Santerre JP, Labow RS. Changes in macrophage function and morphology due to biomedical polyurethane surfaces undergoing biodegradation. J Cell Physiol. 2004; 199(1):8–19. [PubMed: 14978730]
10. Muzykantov VR. Targeting of superoxide dismutase and catalase to vascular endothelium. J Control Release. 2001; 71(1):1–21. [PubMed: 11245904]
11. Abrescia P, Golino P. Free radicals and antioxidants in cardiovascular diseases. Expert Rev Cardiovasc Ther. 2005; 3(1):159–171. [PubMed: 15723584]
12. Dhalla NS, Temsah RM, Netticadan T. Role of oxidative stress in cardiovascular diseases. J Hypertens. 2000; 18(6):655–673. [PubMed: 10872549]
13. Griendling KK, FitzGerald GA. Oxidative stress and cardiovascular injury: part II: animal and human studies. Circulation. 2003; 108(17):2034–2040. [PubMed: 14581381]
14. Farb A, Burke AP, Kolodgie FD, Virmani R. Pathological mechanisms of fatal late coronary stent thrombosis in humans. Circulation. 2003; 108(14):1701–1706. [PubMed: 14504181]
15. Griendling KK, Ushio-Fukai M. Redox control of vascular smooth muscle proliferation. J Lab Clin Med. 1998; 132(1):9–15. [PubMed: 9665366]
16. Szocs K, Lassegue B, Sorescu D, Hilenski LL, Valppu L, Couse TL, et al. Upregulation of Nox-based NAD(P)H oxidases in restenosis after carotid injury. Arterioscler Thromb Vasc Biol. 2002; 22(1):21–27. [PubMed: 11788456]
17. Pi Y, Zhang LL, Li BH, Guo L, Cao XJ, Gao CY, et al. Inhibition of reactive oxygen species generation attenuates TLR4-mediated proinflammatory and proliferative phenotype of vascular smooth muscle cells. Lab Invest. 2013; 93(8):880–887. [PubMed: 23774581]
18. Yang SC, Bhide M, Crispe IN, Pierce RH, Murthy N. Polyketal copolymers: a new acid-sensitive delivery vehicle for treating acute inflammatory diseases. Bioconjug Chem. 2008; 19(6):1164–1169. [PubMed: 18500834]
19. Tikekar RV, Hernandez M, Land DP, Nitin N. "Click chemistry" based conjugation of lipophilic curcumin to hydrophilic ε-polylysine for enhanced functionality. Food Res Int. 2013; 54(1):44–47.
20. Ren J, Li Q, Dong F, Feng Y, Guo Z. Phenolic antioxidants-functionalized quaternized chitosan: Synthesis and antioxidant properties. Int J Biol Macromol. 2013; 53:77–81. [PubMed: 23164754]
21. Dobrun LA, Kuzyakina EL, Rakitina OV, Sergeeva OY, Mikhailova ME, Domnina NS, et al. Molecular characteristics and antioxidant activity of polyethylene glycols modified by sterically hindered phenols. J Struct Chem. 2011; 52(6):1161–1166.
22. Hu P, Tirelli N. Scavenging ROS: superoxide dismutase/catalase mimetics by the use of an oxidation-sensitive nanocarrier/enzyme conjugate. Bioconjug Chem. 2012; 23(3):438–449. [PubMed: 22292618]
23. Phuong Thu H, Thi Minh Nguyet T, Hong Duong P, Quang Huan N, Xuan Phuc N. The synthesis of poly(lactide)-vitamin E TPGS (PLA-TPGS) copolymer and its utilization to formulate a curcumin nanocarrier. Adv Nat Sci: Nanosci Nanotechnol. 2010; 1(1):015012.
24. Spizzirri UG, Iemma F, Puoci F, Cirillo G, Curcio M, Parisi OI, et al. Synthesis of antioxidant polymers by grafting of gallic acid and catechin on gelatin. Biomacromolecules. 2009; 10(7): 1923–1930. [PubMed: 19413362]
25. Williams SR, Lepene BS, Thatcher CD, Long TE. Synthesis and characterization of poly(ethylene glycol)-glutathione conjugate self-assembled nanoparticles for antioxidant delivery. Biomacromolecules. 2009; 10(1):155–161. [PubMed: 19086778]
26. Wang Y, Singh A, Xu P, Pindrus MA, Blasioli DJ, Kaplan DL. Expansion and osteogenic differentiation of bone marrow-derived mesenchymal stem cells on a vitamin C functionalized polymer. Biomaterials. 2006; 27(17):3265–3273. [PubMed: 16494940]
27. Wattamwar PP, Mo Y, Wan R, Palli R, Zhang Q, Dziubla TD. Antioxidant activity of degradable polymer poly(trolox ester) to suppress oxidative stress injury in the cells. Adv Funct Mater. 2010; 20(1):147–154.
28. Motlagh D, Allen J, Hoshi R, Yang J, Lui K, Ameer G. Hemocompatibility evaluation of poly(diol citrate) in vitro for vascular tissue engineering. J Biomed Mater Res A. 2007; 82A(4):907–916. [PubMed: 17335023]

29. Kibbe MR, Martinez J, Popowich DA, Kapadia MR, Ahanchi SS, Aalami OO, et al. Citric acid-based elastomers provide a biocompatible interface for vascular grafts. J Biomed Mater Res A. 2010; 93(1):314–324. [PubMed: 19569210]
30. Hoshi RA, Van Lith R, Jen MC, Allen JB, Lapidos KA, Ameer G. The blood and vascular cell compatibility of heparin-modified ePTFE vascular grafts. Biomaterials. 2013; 34(1):30–41. [PubMed: 23069711]
31. Sharma AK, Bury MI, Fuller NJ, Marks AJ, Kollhoff DM, Rao MV, et al. Cotransplantation with specific populations of spina bifida bone marrow stem/progenitor cells enhances urinary bladder regeneration. Proc Natl Acad Sci U S A. 2013; 110(10):4003–4008. [PubMed: 23431178]
32. Wang Y-C, Chuang Y-C, Ku Y-H. Quantitation of bioactive compounds in citrus fruits cultivated in Taiwan. Food Chemistry. 2007; 102(4):1163–1171.
33. Akbıyık T, Sönmezoğlu İ, Güçlü K, Tor İ, Apak R. Protection of ascorbic acid from coppeRII) −catalyzed oxidative degradation in the presence of fruit acids: citric, oxalic, tartaric, malic, malonic, and fumaric acids. Int J Food Prop. 2011; 15(2):398–411.
34. Ahmad I, Ali Sheraz M, Ahmed S, Shad Z, Vaid FHM. Photostabilization of ascorbic acid with citric acid, tartaric acid and boric acid in cream formulations. Int J Cosmet Sci. 2012; 34(3):240–245. [PubMed: 22296174]
35. Day SM, Duquaine D, Mundada LV, Menon RG, Khan BV, Rajagopalan S, et al. Chronic iron administration increases vascular oxidative stress and accelerates arterial thrombosis. Circulation. 2003; 107(20):2601–2606. [PubMed: 12732602]
36. Kell DB. Iron behaving badly: inappropriate iron chelation as a major contributor to the aetiology of vascular and other progressive inflammatory and degenerative diseases. BMC Med Genomics. 2009; 2:2. [PubMed: 19133145]
37. Cai L, Koropatnick J, Cherian MG. Roles of vitamin C in radiation-induced DNA damage in presence and absence of copper. Chem Biol Interact. 2001; 137(1):75–88. [PubMed: 11518565]
38. Sperling LH. Introduction to Physical Polymer Science (4th Edition). 2006:1–845.
39. Prieto MA, Rodríguez-Amado I, Vázquez JA, Murado MA. β-carotene assay revisited. Application to characterize and quantify antioxidant and prooxidant activities in a microplate. J Agric Food Chem. 2012; 60(36):8983–8993. [PubMed: 22849655]
40. Loor G, Kondapalli J, Schriewer JM, Chandel NS, Vanden Hoek TL, Schumacker PT. Menadione triggers cell death through ROS-dependent mechanisms involving PARP activation without requiring apoptosis. Free Radic Biol Med. 2010; 49(12):1925–1936. [PubMed: 20937380]
41. Yang J, Webb AR, Ameer GA. Novel citric acid-based biodegradable elastomers for tissue engineering. Adv Mater. 2004; 16(6):511–516.
42. Zhao H, Serrano MC, Popowich DA, Kibbe MR, Ameer GA. Biodegradable nitric oxide-releasing poly(diol citrate) elastomers. J Biomed Mater Res A. 2010; 93(1):356–363. [PubMed: 19569216]
43. Yohannan Panicker C, Tresa Varghese H, Philip D. FT-IR, FT-Raman and SERS spectra of vitamin C. Spectrochim Acta A Mol Biomol Spectrosc. 2006; 65(3–4):802–804. [PubMed: 16530470]
44. Gil MI, Tomas-Barberan FA, Hess-Pierce B, Holcroft DM, Kader AA. Antioxidant activity of pomegranate juice and its relationship with phenolic composition and processing. J Agric Food Chem. 2000; 48(10):4581–4589. [PubMed: 11052704]
45. Serrano MC, Carbajal L, Ameer GA. Novel biodegradable shape-memory elastomers with drug-releasing capabilities. Adv Mater. 2011; 23(19):2211–2215. [PubMed: 21557337]
46. Torday JS, Torday DP, Gutnick J, Qin J, Rehan V. Biologic role of fetal lung fibroblast triglycerides as antioxidants. Pediatr Res. 2001; 49(6):843–849. [PubMed: 11385147]
47. Lynch SR, Cook JD. Interaction of vitamin C and iron. Ann N Y Acad Sci. 1980; 355:32–44. [PubMed: 6940487]
48. Gregory EK, Vavra AK, Moreira ES, Havelka GE, Jiang Q, Lee VR, et al. Antioxidants modulate the antiproliferative effects of nitric oxide on vascular smooth muscle cells and adventitial fibroblasts by regulating oxidative stress. Am J Surg. 2011; 202(5):536–540. [PubMed: 21944289]
49. Ivanova IP, Trofimova SV, Piskarev IM. Evaluation of prooxidant properties of ascorbic acid. Biophysics. 2013; 58(4):453–456.

50. Ulrich-Merzenich G, Metzner C, Schiermeyer B, Vetter H. Vitamin C and vitamin E antagonistically modulate human vascular endothelial and smooth muscle cell DNA synthesis and proliferation. Eur J Nutr. 2002; 41(1):27–34. [PubMed: 11990005]
51. Wang H, Joseph JA. Quantifying cellular oxidative stress by dichlorofluorescein assay using microplate reader. Free Radic Biol Med. 1999; 27(5–6):612–616. [PubMed: 10490282]
52. Yang W, de Bono DP. A new role for vascular endothelial growth factor and fibroblast growth factors: increasing endothelial resistance to oxidative stress. FEBS Lett. 1997; 403(2):139–142. [PubMed: 9042954]
53. Smith AR, Visioli F, Hagen TM. Vitamin C matters: increased oxidative stress in cultured human aortic endothelial cells without supplemental ascorbic acid. Faseb j. 2002; 16(9):1102–1104. [PubMed: 12039848]
54. Criddle DN, Gillies S, Baumgartner-Wilson HK, Jaffar M, Chinje EC, Passmore S, et al. Menadione-induced reactive oxygen species generation via redox cycling promotes apoptosis of murine pancreatic acinar cells. J Biol Chem. 2006; 281(52):40485–40492. [PubMed: 17088248]
55. May JM, Qu ZC, Li X. Ascorbic acid blunts oxidant stress due to menadione in endothelial cells. Arch Biochem Biophys. 2003; 411(1):136–144. [PubMed: 12590932]
56. Frikke-Schmidt H, Roursgaard M, Lykkesfeldt J, Loft S, Nojgaard JK, Moller P. Effect of vitamin C and iron chelation on diesel exhaust particle and carbon black induced oxidative damage and cell adhesion molecule expression in human endothelial cells. Toxicol Lett. 2011; 203(3):181–189. [PubMed: 21421028]
57. Saigo K, Kono M, Takagi Y, Takenokuchi M, Hiramatsu Y, Tada H, et al. Deferasirox reduces oxidative stress in patients with transfusion dependency. J Clin Med Res. 2013; 5(1):57–60. [PubMed: 23390477]
58. Ikeda Y, Ozono I, Tajima S, Imao M, Horinouchi Y, Izawa-Ishizawa Y, et al. Iron chelation by Deferoxamine prevents renal interstitial fibrosis in mice with unilateral ureteral obstruction. PLoS ONE. 2014; 9(2):e89355. [PubMed: 24586712]
59. Reeder BJ, Hider RC, Wilson MT. Iron chelators can protect against oxidative stress through ferryl heme reduction. Free Radic Biol Med. 2008; 44(3):264–273. [PubMed: 18215735]
60. Khaw KT, Bingham S, Welch A, Luben R, Wareham N, Oakes S, et al. Relation between plasma ascorbic acid and mortality in men and women in EPIC-Norfolk prospective study: A prospective population study. Lancet. 2001; 357(9257):657–663. [PubMed: 11247548]
61. Sesso HD, Buring JE, Christen WG, Kurth T, Belanger C, MacFadyen J, et al. Vitamins E and C in the prevention of cardiovascular disease in men: The physicians' health study II randomized controlled trial. JAMA. 2008; 300(18):2123–2133. [PubMed: 18997197]
62. Tardif J-C, Grégoire J, Schwartz L, Title L, Laramée L, Reeves F, et al. Effects of AGI-1067 and probucol after percutaneous coronary interventions. Circulation. 2003; 107(4):552–558. [PubMed: 12566365]
63. Kuiper KKJ, Salem M, Gudbrandsen OA, Muna ZA, Berge RK, Nordrehaug JE. Dose-dependent coronary artery intimal thickening after local delivery of the anti-oxidant tetradecylthioacetic acid from stents. Atherosclerosis. 2007; 195(1):e39–e47. [PubMed: 17399716]
64. Bräsen JH, Leppänen O, Inkala M, Heikura T, Levin M, Ahrens F, et al. Extracellular superoxide dismutase accelerates endothelial recovery and inhibits in-stent restenosis in stented atherosclerotic Watanabe heritable hyperlipidemic rabbit aorta. J Am Coll Cardiol. 2007; 50(23): 2249–2253. [PubMed: 18061074]
65. Laukkanen MO, Kivelä A, Rissanen T, Rutanen J, Karkkainen MK, Leppanen O, et al. Adenovirus-mediated extracellular superoxide dismutase gene therapy reduces neointima formation in balloon-denuded rabbit aorta. Circulation. 2002; 106(15):1999–2003. [PubMed: 12370226]
66. Forbes SP, Alferiev IS, Chorny M, Adamo RF, Levy RJ, Fishbein I. Modulation of NO and ROS production by AdiNOS transduced vascular cells through supplementation with L-Arg and BH4: Implications for gene therapy of restenosis. Atherosclerosis. 2013; 230(1):23–32. [PubMed: 23958248]
67. Drouin G, Godin JR, Page B. The genetics of vitamin C loss in vertebrates. Curr Genomics. 2011; 12(5):371–378. [PubMed: 22294879]

68. Ivanov VO, Ivanova SV, Niedzwiecki A. Ascorbate affects proliferation of guinea-pig vascular smooth muscle cells by direct and extracellular matrix-mediated effects. J Mol Cell Cardiol. 1997; 29(12):3293–3303. [PubMed: 9441835]

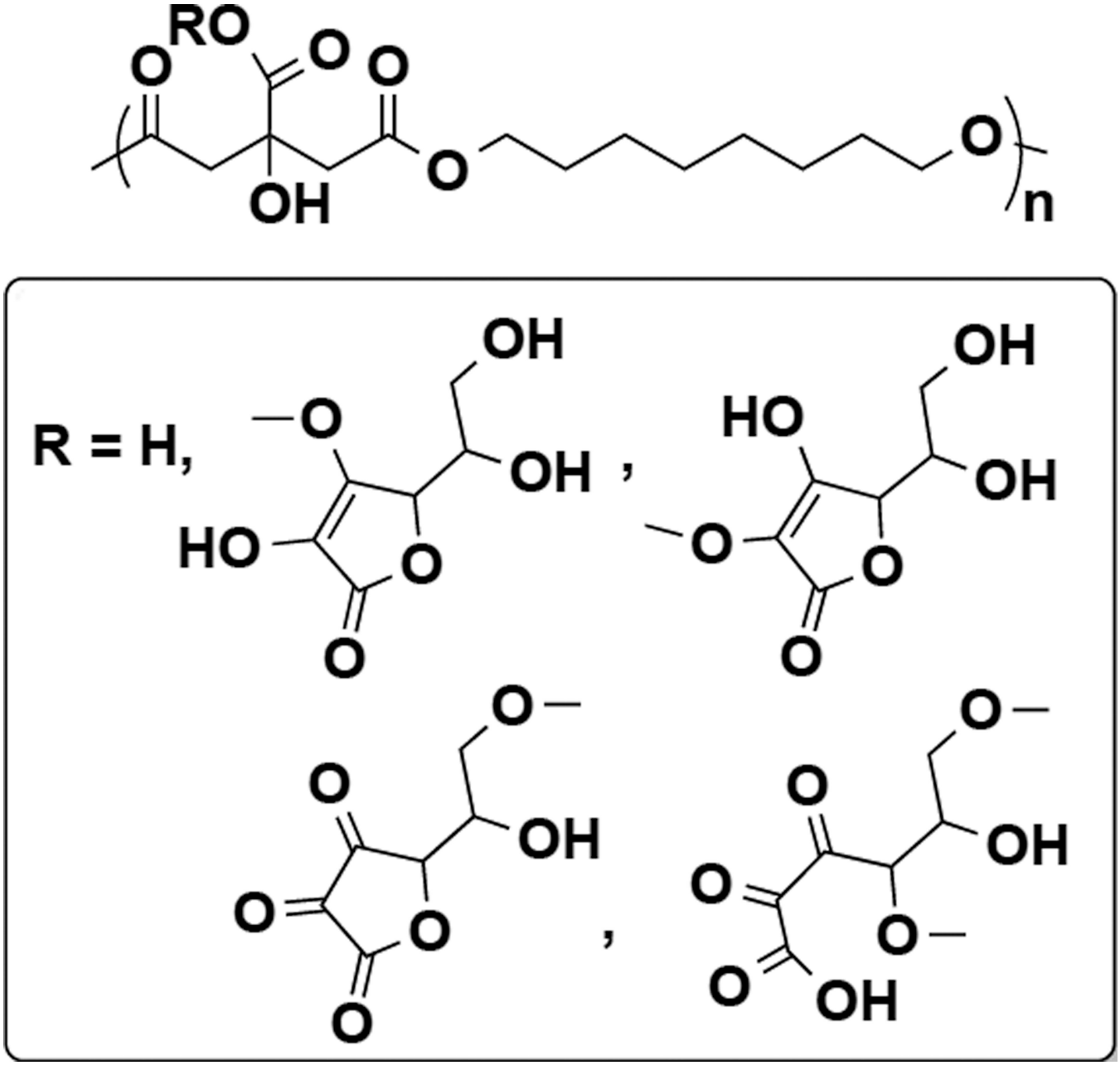

Figure 1.
Proposed structure and scheme of poly(1,8-octanediol-co-citrate-co-ascorbate) (POCA). In case of R=H, the copolymer is poly(1,8-octanediol-co-citrate)(POC).

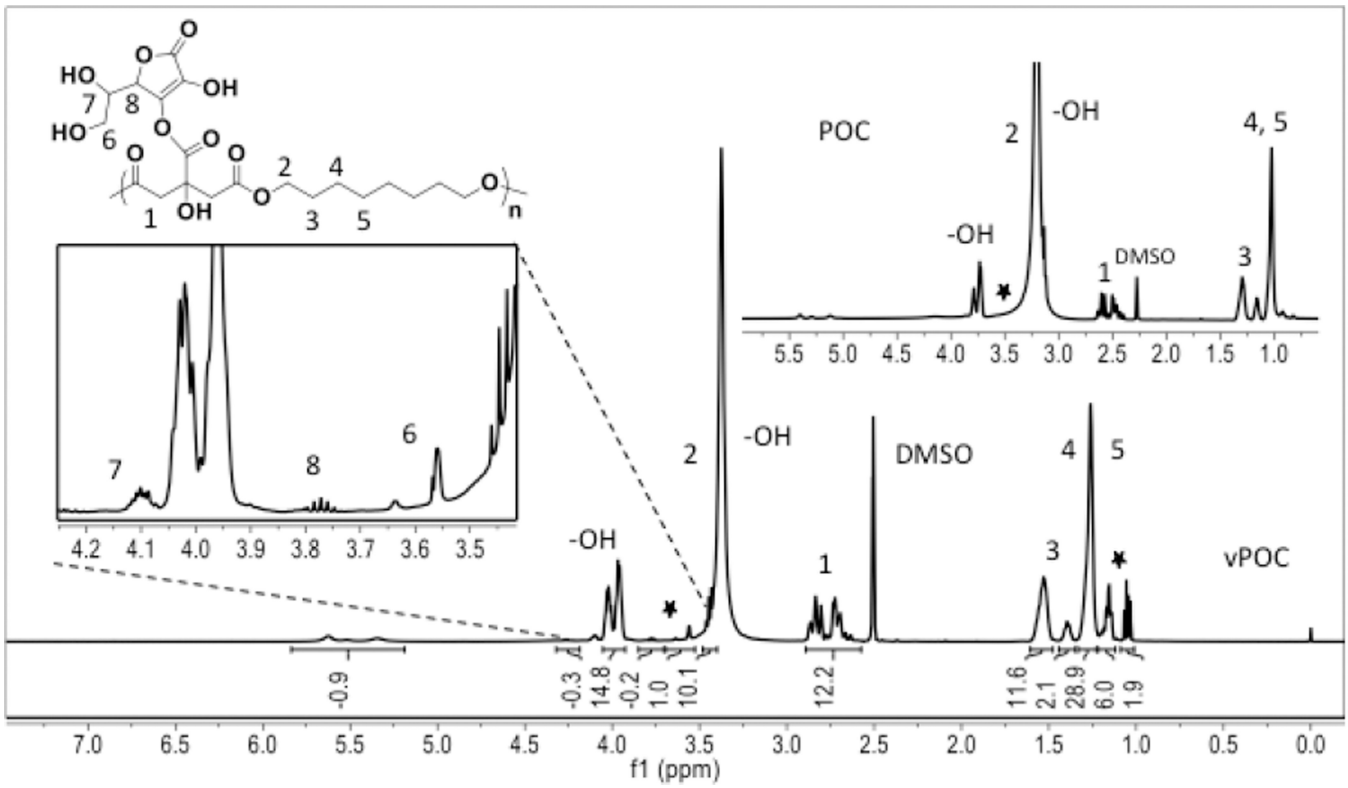

Figure 2.

^{1}H NMR spectra of poly(octanediol-co-citrate-co-ascorbate) (POCA) and poly(octanediol-co-citrate) (POC) (insert) in DMSO-*d*

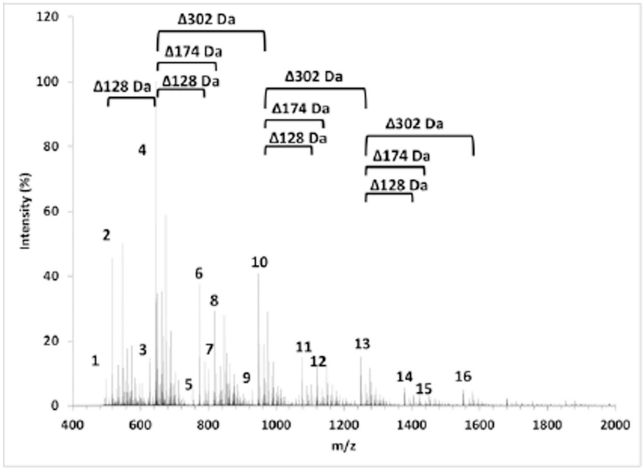

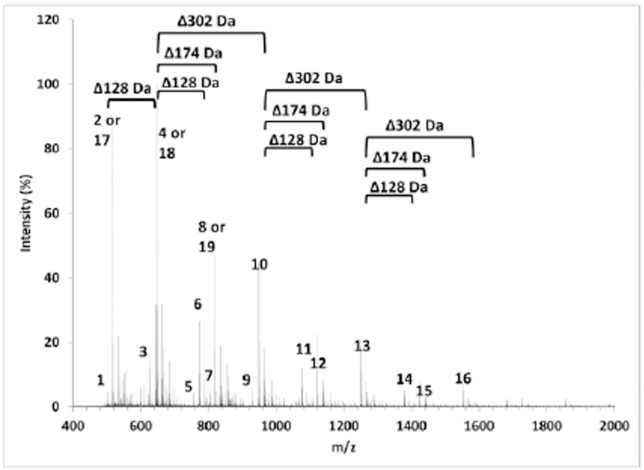

#	Structure	Expected m/z	Measured m/z
1	Cyclic C_2D_1 +Na^+	499.43	499.85
2	C_2D_1 +Na^+	517.44	517.65
3	Cyclic C_2D_2 +Na^+	627.64	627.88
4	C_2D_2 +Na^+	645.65	645.82
5	Cyclic C_2D_3 +Na^+	755.86	756.07
6	C_2D_3 +Na^+	773.87	773.99
7	Cyclic C_3D_2 +Na^+	801.75	802.12
8	C_3D_2 +Na^+	819.76	819.89
9	Cyclic C_3D_3 +Na^+	929.97	930.15
10	C_3D_3 +Na^+	947.98	948.05
11	C_3D_4 +Na^+	1076.19	1076.22
12	C_4D_3 +Na^+	1122.09	1122.12
13	C_4D_4 +Na^+	1250.3	1250.29
14	C_4D_5 +Na^+	1378.52	1378.63
15	C_5D_4 +Na^+	1424.41	1424.53
16	C_5D_5 +Na^+	1552.63	1552.73
17	$C_1D_1A_1$ +K^+	517.54	517.65
18	$C_1D_2A_1$ +K^+	645.76	645.82
19	$C_2D_2A_1$ +K^+	819.87	819.89

$C_nD_nA_n$ stands for co-oligomers of n segments of citrate (C), octanediol (D) and Ascorbic acid (A).

Figure 3.

MALDI spectra of poly(octanediol-co-citrate) (POC, top left) and poly(octanediol-co-citrate-co-ascorbate) (POCA, bottom left) prepolymers. Table, right, shows identified oligomer peaks and clusters.

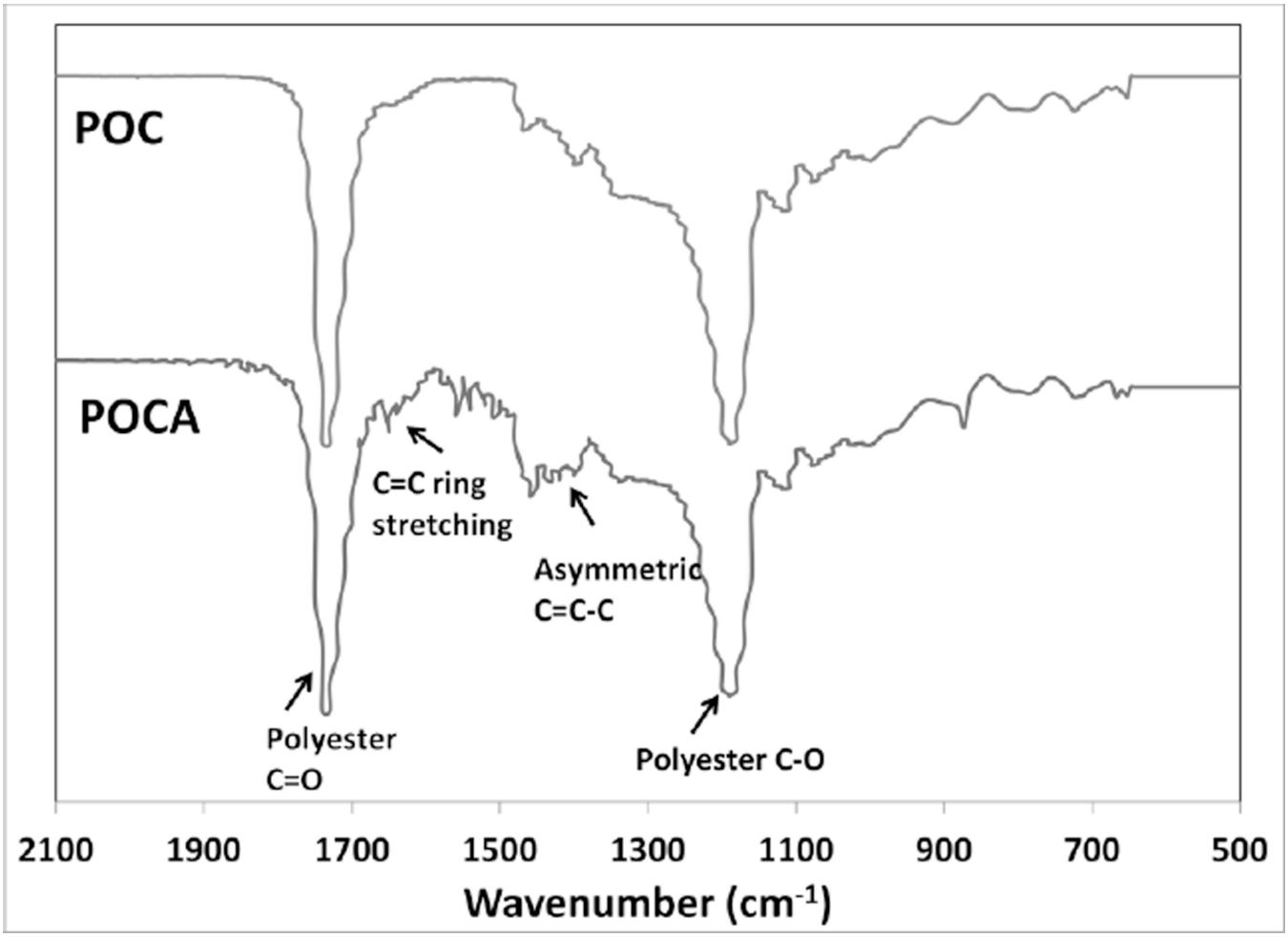

Figure 4.

FTIR spectra of poly(octanediol-co-citrate)(POC) and poly(octanediol-co-citrate-co-ascorbate) (POCA) polymers, using attenuated total reflectance FTIR on polymer films.

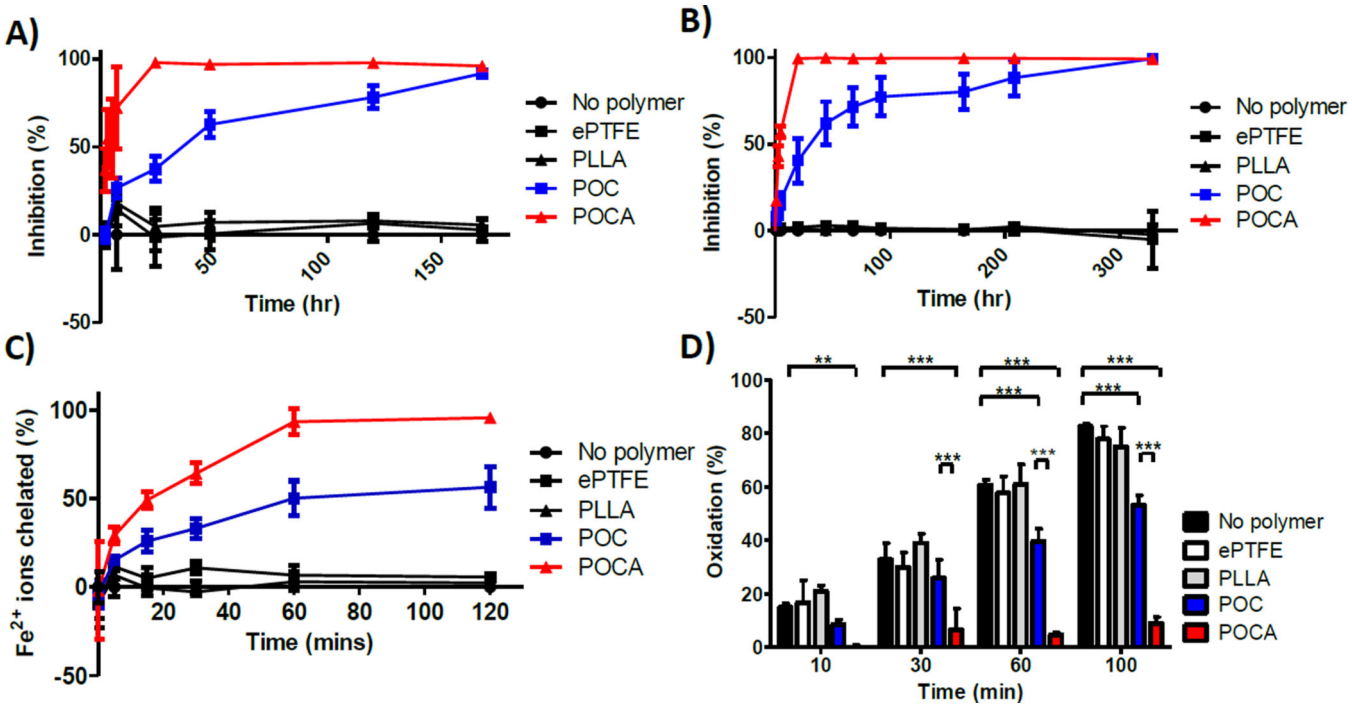

Figure 5.

DPPH (A) and ABTS (B) assay show free radical inhibition by both POC and POCA, whereas PLLA and ePTFE have no radical scavenging activity. POC and POCA both chelate iron ions, with POCA exhibiting stronger chelation (C). POC and POCA both inhibit lipid peroxidation, while ePTFE and PLLA do not have any effect on lipid peroxidation. N≥3, Mean ± SD. *p<0.05 **p<0.01, ***p<0.001

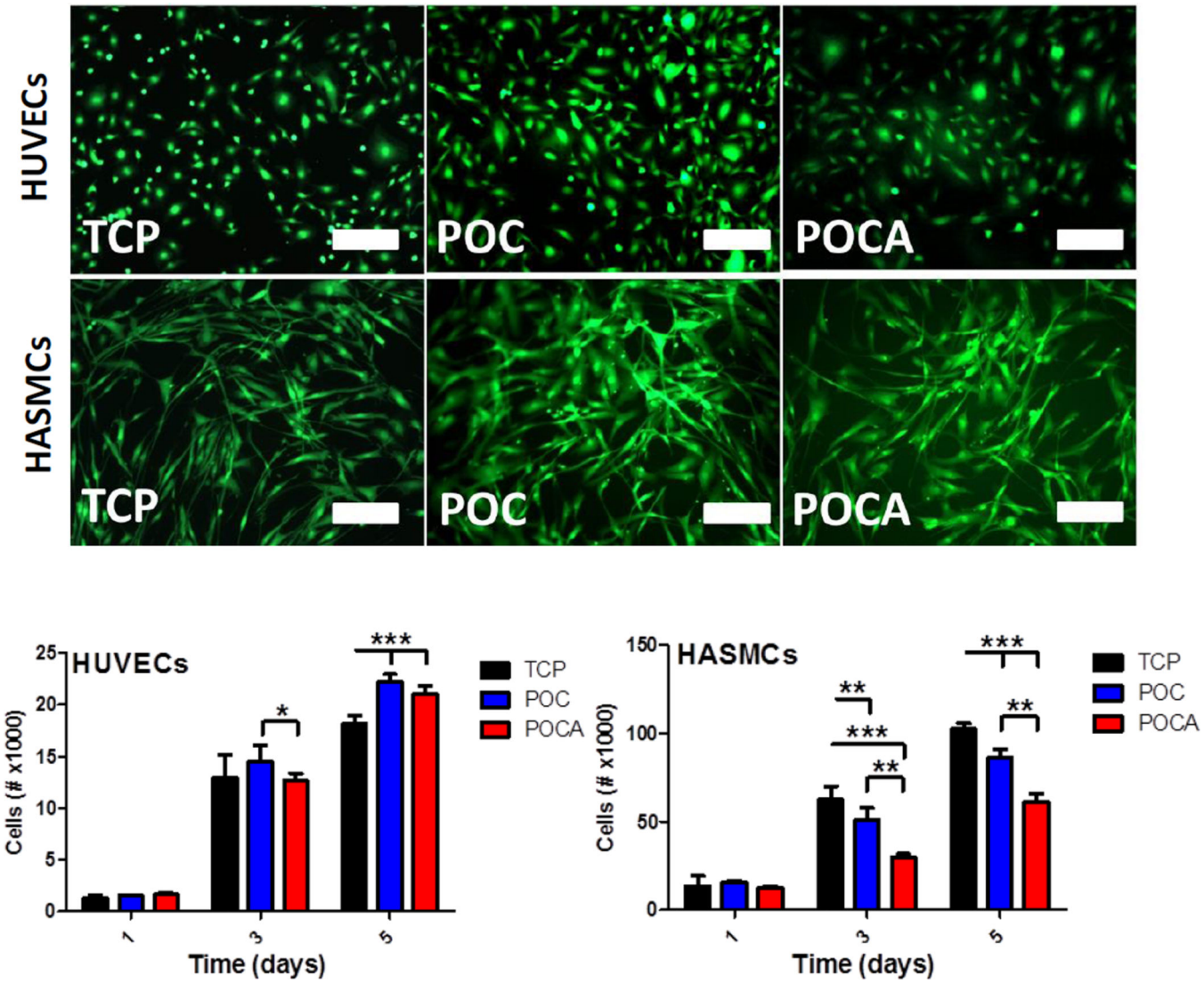

Figure 6.

Top: POC and POCA are compatible with vascular cells, showing high viability after 5 days of culture on polymer-coated TCP plates. Note: ethidium homodimer stain omitted due to strong adherence of fluorophore to polymer substrates. Bar=100 um. Bottom: POC and POCA both support HUVEC proliferation, while POC and to a larger extent POCA inhibit HASMC proliferation. N≥3, Mean ± SD. *p<0.05 **p<0.01, ***p<0.001

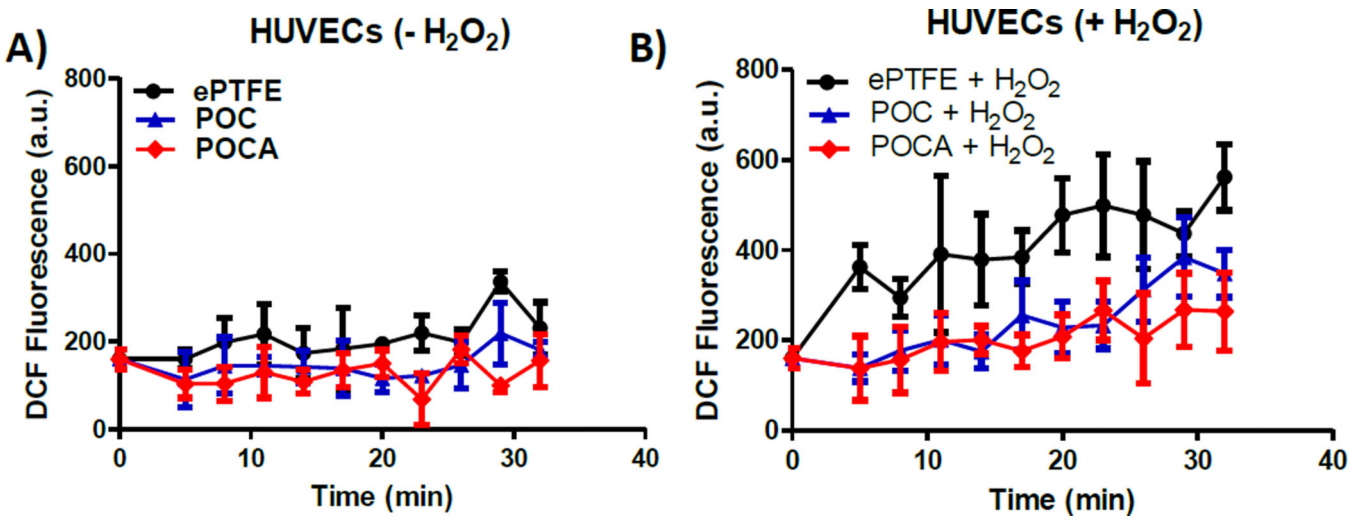

Figure 7.

HUVECs exposed to POC and POCA are resistant to oxidative stress. A) Without H_2O_2 challenge, POC and POCA both reduced basal oxidative stress levels in HUVECS (P=0.012 and 0.008 for ePTFE vs. POC and ePTFE vs. POCA, respectively). B) After H_2O_2 challenge, both polymers provided protection from increasing levels of oxidative stress (P=0.013 and 0.007 for ePTFE vs. POC and ePTFE vs. POCA, respectively). N≥3, Mean ± SD.

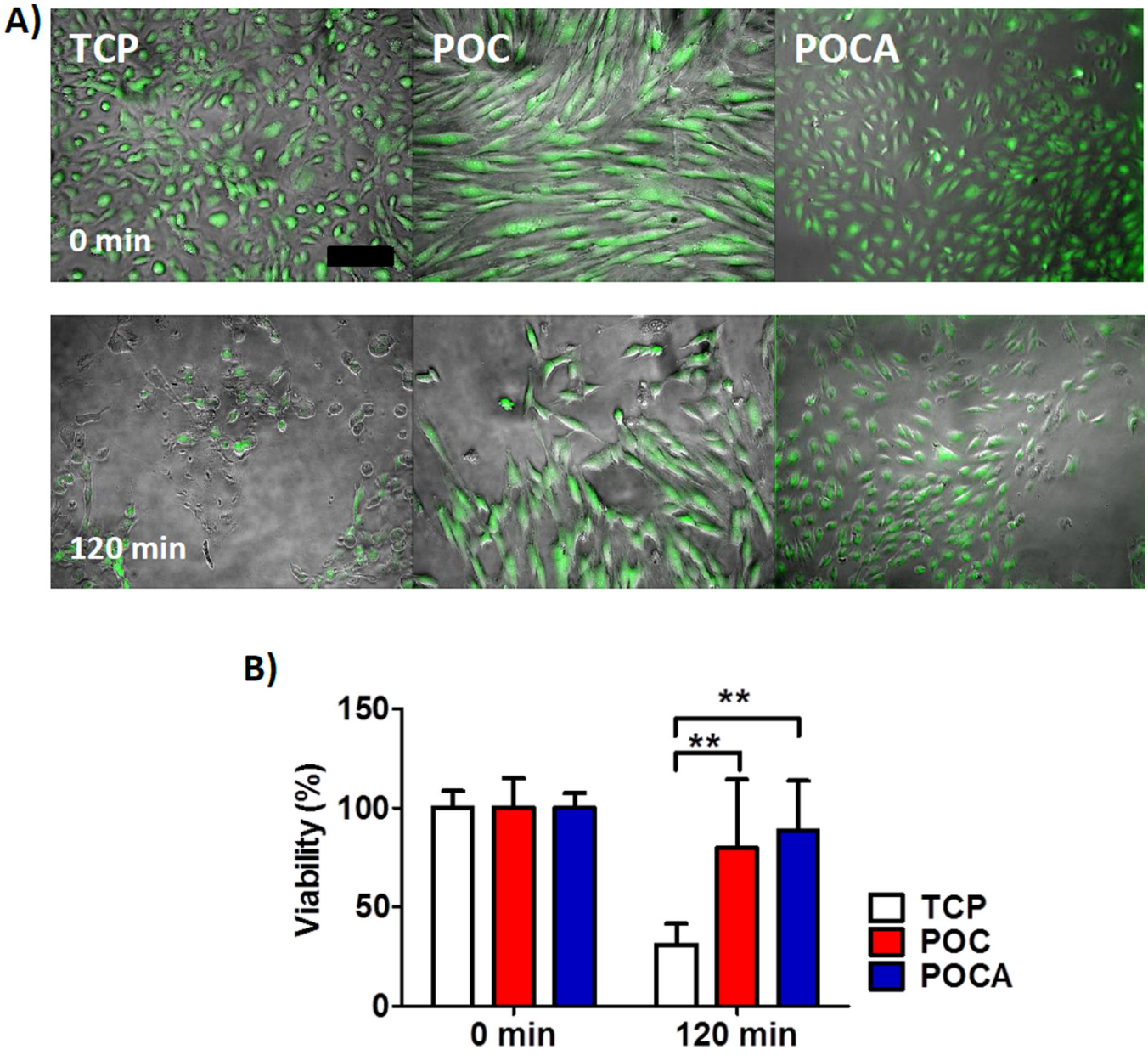

Figure 8.

HUVECs cultured on top of POC and POCA showed prolonged survival upon menadione stimulation for 120 minutes. POC and POCA provided protection from excessive ROS-induced cell death. A) Combined overlap image of contrast light microscopy with fluorescent image shown. Green indicates calcein AM stain for live cells. Bar=200 μm. B) Quantification of percentage of calcein AM positive cells after 120 minutes relative to unchallenged cells. N=4, Mean ± S.D., ** P<0.01.

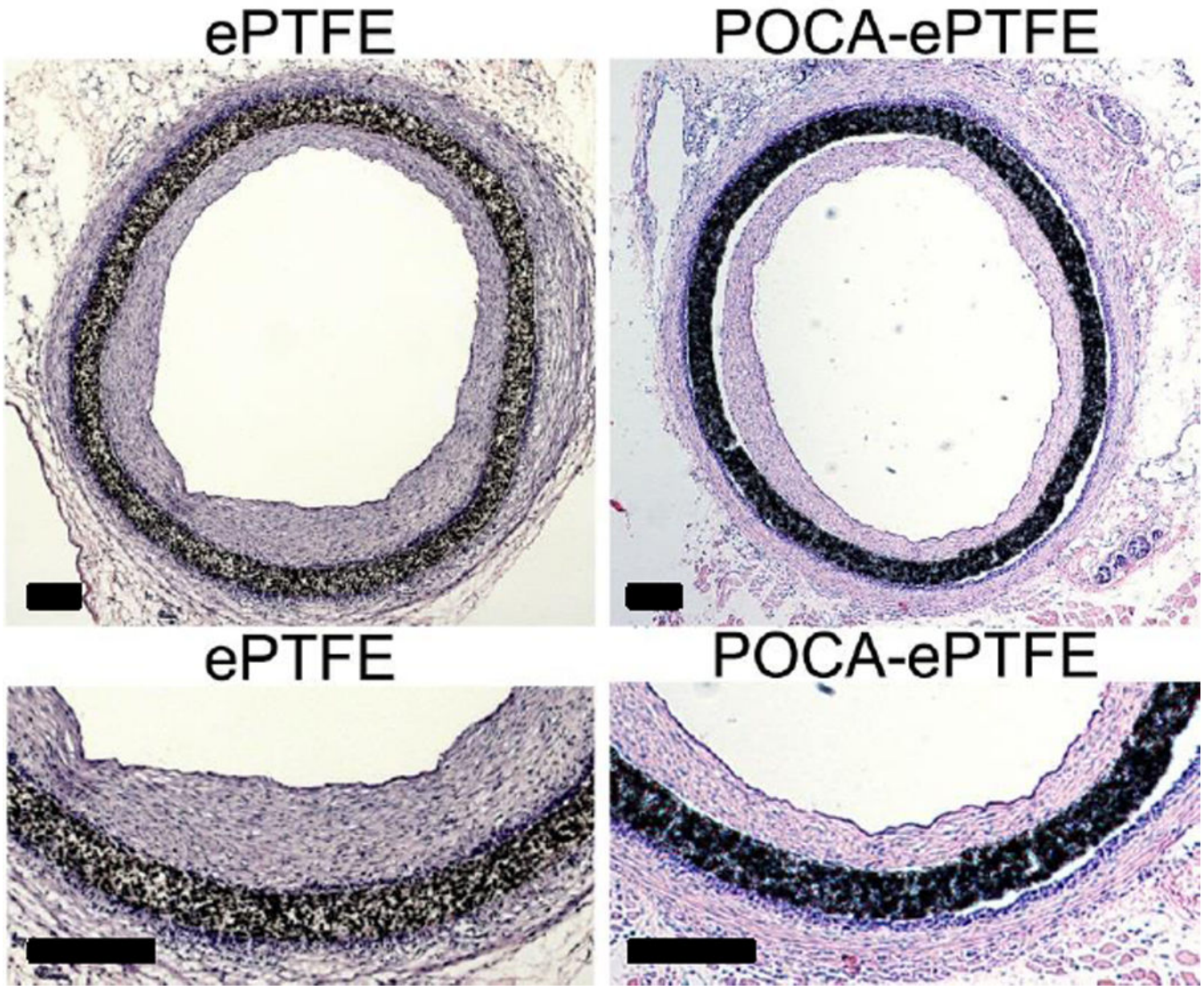

Figure 9.

POCA-coated ePTFE grafts show reduced intimal hyperplasia compared to regular ePTFE grafts in a guinea pig aortic graft interposition model after 4 weeks of implantation. Bar=200 μm.

Table 1

Mechanical and physical properties of synthesized POC and POCA

Polymer	ρ (g m^{-3}) × 10^{-6}	Young's modulus (Mpa)	Maximum Load (N)	n (mol m^{-3})	M_c (g mol^{-1})
POC	1.23±0.167	2.12±0.18	1.64±0.06	288.84±23.84	4258±677
POCA	1.43±0.267	2.24±0.22	1.59±0.33	305.19±29.97	4686±989

ρ: polymer density; n: number of active network chain segments per unit volume; M_C: molecular weight between crosslinks; post-polymerization for 4 days at 80°C